eLIFE elifesciences.org

RESEARCH ARTICLE

Figures and figure supplements

Stimulus vignetting and orientation selectivity in human visual cortex

Zvi N Roth *et al*

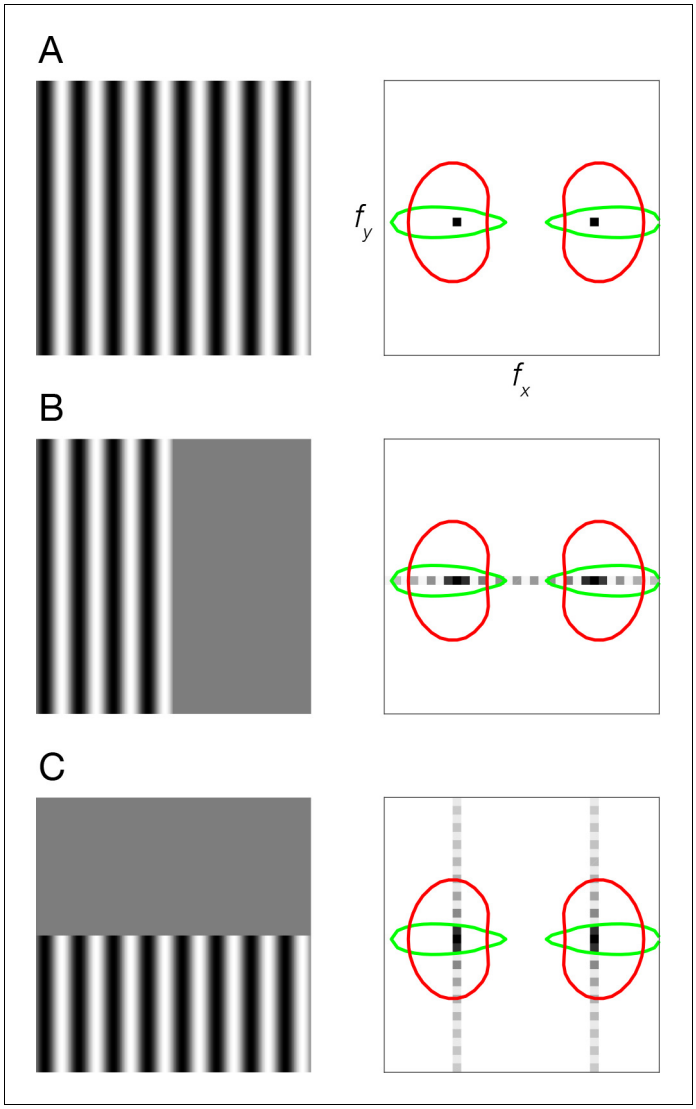

Figure 1. Stimulus vignetting. (**A**) Stimulus image (left) and Fourier amplitude (right) for sinusoidal grating that is infinite in extent. Black dots, Fourier amplitude restricted to a single spatial frequency and orientation component. Colored ovals, orientation tuning (polar angle cross-section through the oval) and spatial frequency tuning (radial cross-section) of two hypothetical V1 neurons. Red oval, neuron with broad orientation tuning and narrow spatial frequency tuning. Green oval, neuron with narrow orientation tuning and broad spatial frequency tuning. (**B**) Sinusoidal grating vignetted by vertical aperture. Light gray dots, spread of Fourier energy because of the aperture. (**C**) Sinusoidal grating vignetted by horizontal aperture.

DOI: https://doi.org/10.7554/eLife.37241.002

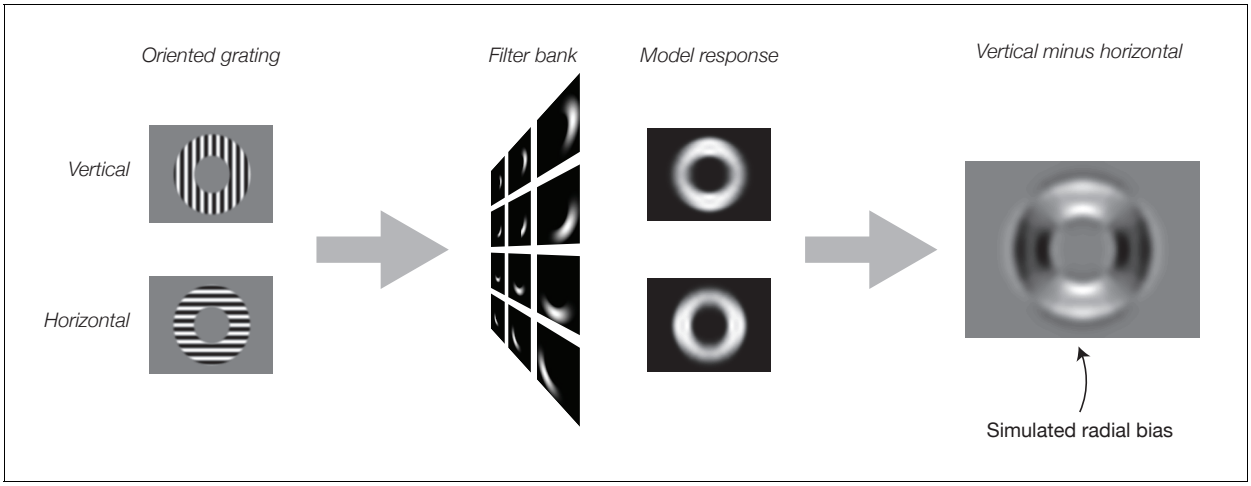

Figure 2. Simulated neural responses illustrating the impact of stimulus vignetting. Oriented gratings were vignetted by inner and outer annuli, using stimulus parameters identical to those from ***Freeman et al. (2011)***. Next, the gratings were used as input to the model. Model responses were computed separately for vertical (top) and horizontal (bottom) gratings. Finally, model output was computed as the responses to vertical minus responses to horizontal gratings. Model exhibits a preference for horizontal gratings along the horizontal meridian and a preference for vertical gratings along the vertical meridian (i.e. a radial bias).

DOI: https://doi.org/10.7554/eLife.37241.003

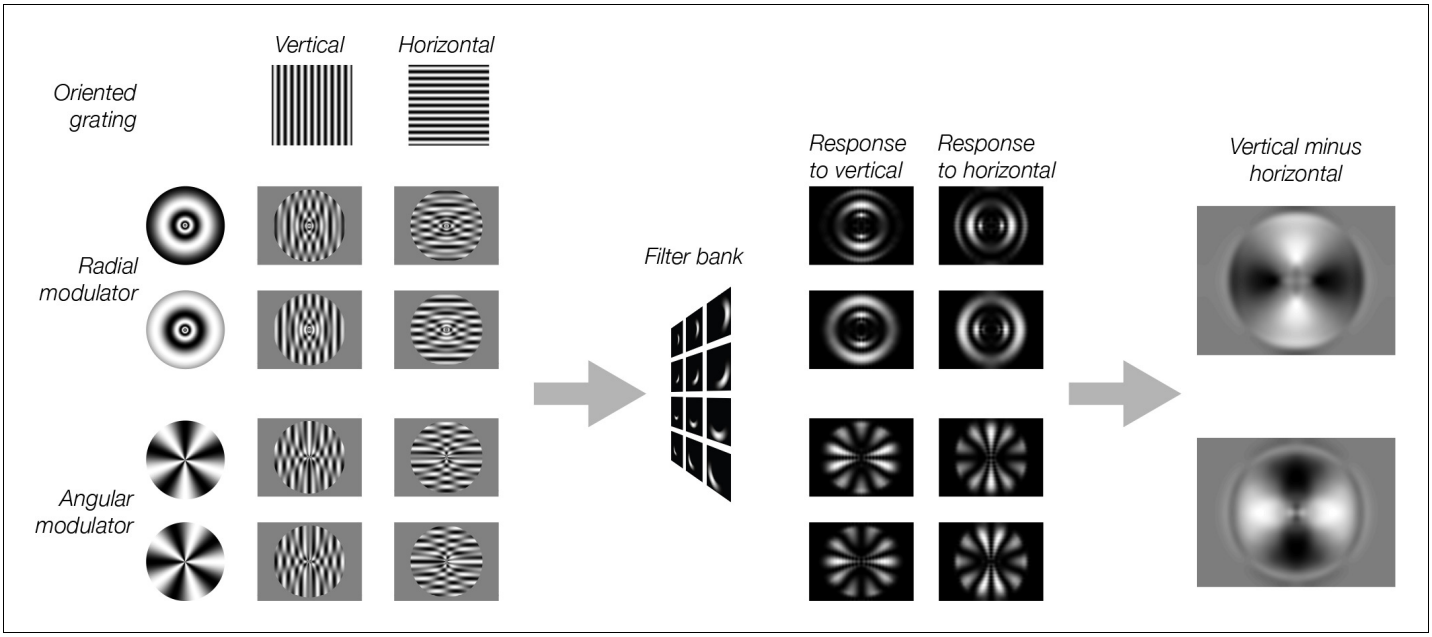

Figure 3. Model predictions for modulated gratings. Each of the eight stimuli were created by multiplying a vertical or horizontal grating by a radial or angular modulator. These stimuli were used as input to the model. Model responses were computed as in ***Figure 2***. For radial modulated gratings (top two rows), the model exhibits a radial preference: larger responses to horizontal gratings along the horizontal meridian, larger responses to vertical gratings along the vertical meridian. However, for angular modulated gratings (bottom two rows), the orientation preference is tangential: larger responses for horizontal gratings along the vertical meridian and larger responses for vertical gratings along the horizontal meridian.

DOI: https://doi.org/10.7554/eLife.37241.004

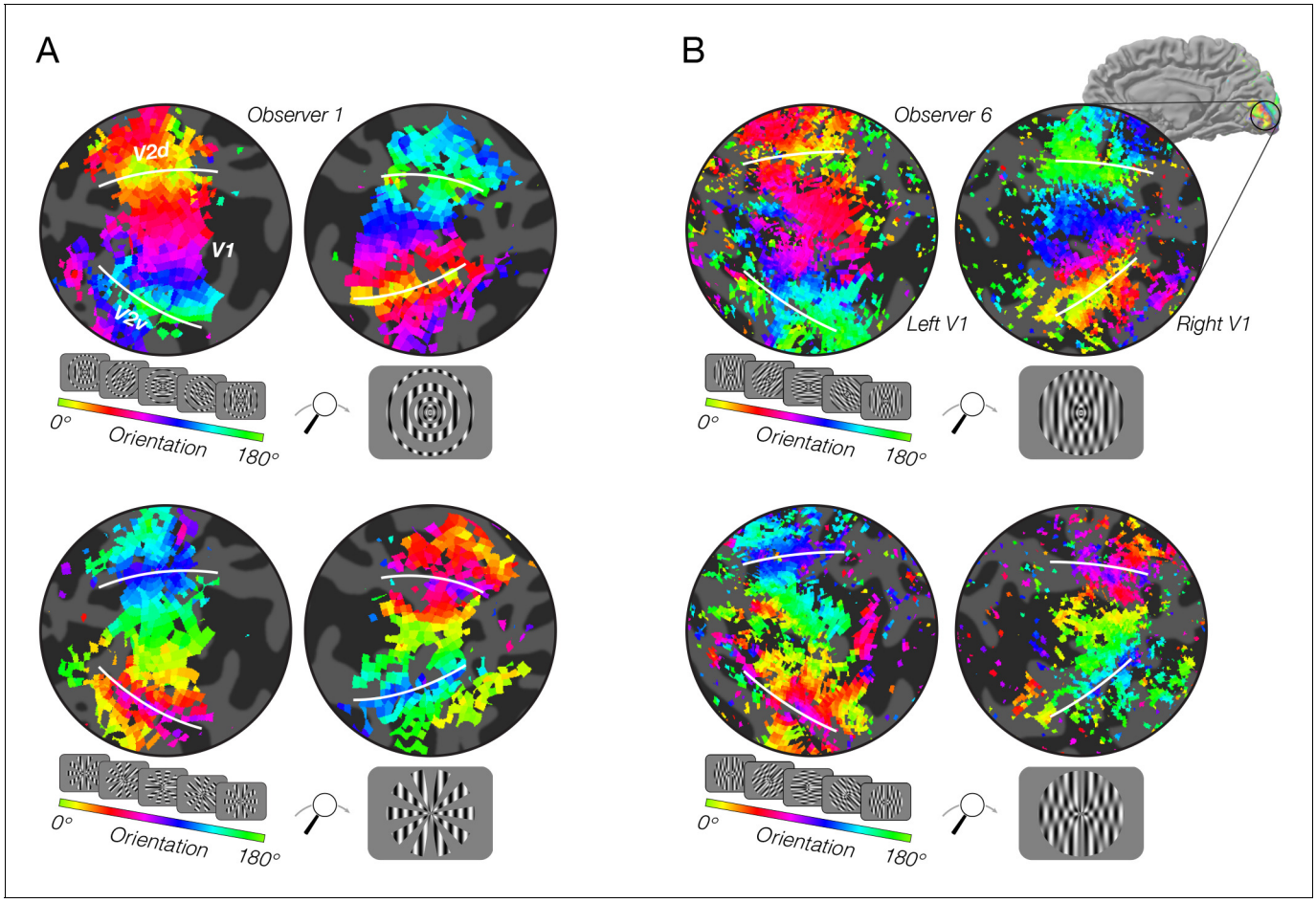

Figure 4. fMRI measurements of orientation bias depend on stimulus vignetting. (**A**) Conventional resolution, 3T. Top: Responses to phase-encoded oriented gratings multiplied by a static radial modulator (shown in inset). The oriented grating cycled through 16 steps of orientation ranging from 0˚ to 180˚ every 24 s. The radial modulator was constant during the entire experiment. Map thresholded at coherence of 0.2. Hue indicates phase of the best fitting sinusoid. White lines indicate V1/V2 boundaries. Bottom: Responses to the same oriented grating as in A, but here the grating is multiplied by an angular modulator. As predicted by the model, the radial modulator gave rise to a radial orientation bias, while the angular modulator gave rise to a tangential orientation bias. (**B**) High-resolution, high field strength (7T) measurements of orientation preference for radial and angular modulators. Stimuli and conventions same as for A, except the modulators were radial and angular sinusoids.

DOI: https://doi.org/10.7554/eLife.37241.005

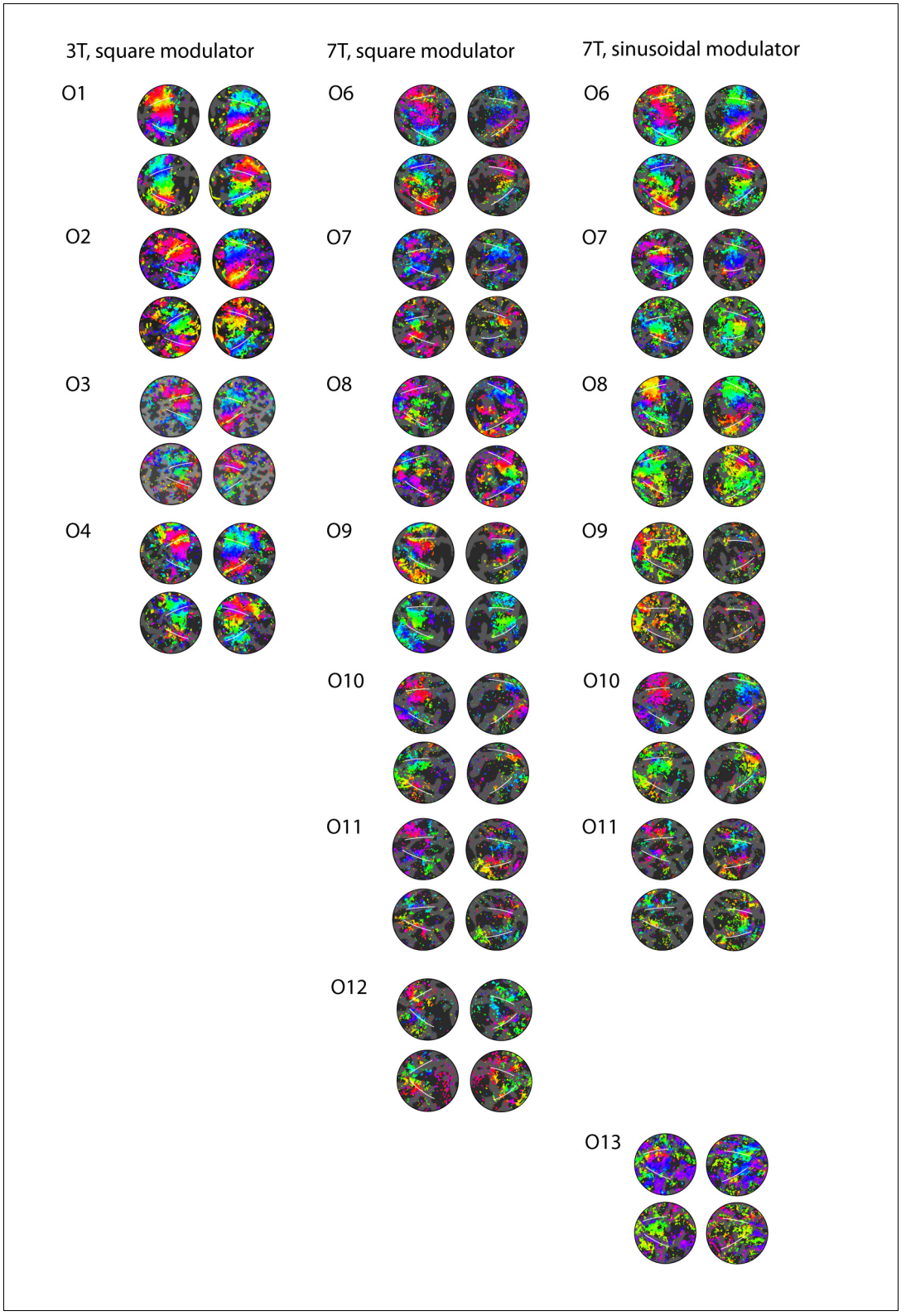

Figure 4—figure supplement 1. fMRI responses for all individual subjects. Left: responses to square wave modulators at 3T. Middle: responses to square wave modulators at 7T. Right: responses to sinusoidal modulators at 7T.

DOI: https://doi.org/10.7554/eLife.37241.006

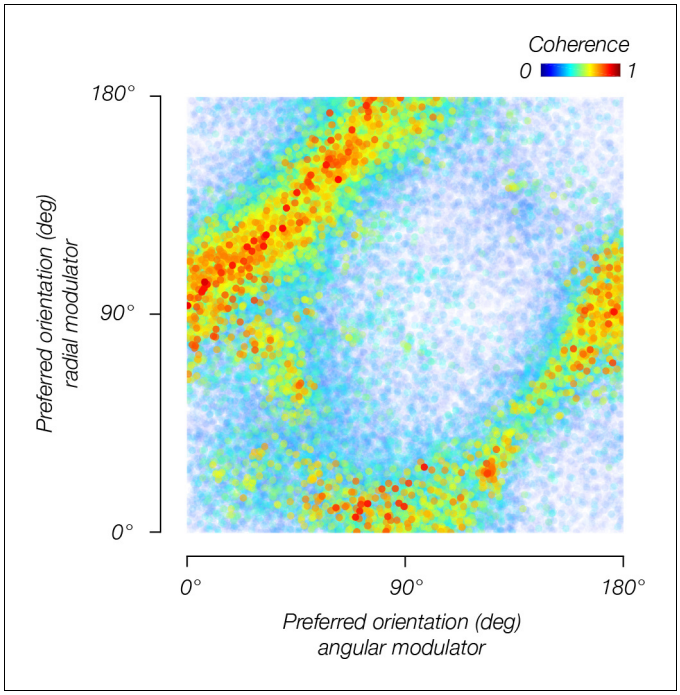

Figure 5. Orientation bias depends on the modulator. Orientation bias for V1 voxels pooled across observers for the angular modulator (y-axis) and radial modulator (x-axis).
DOI: https://doi.org/10.7554/eLife.37241.007

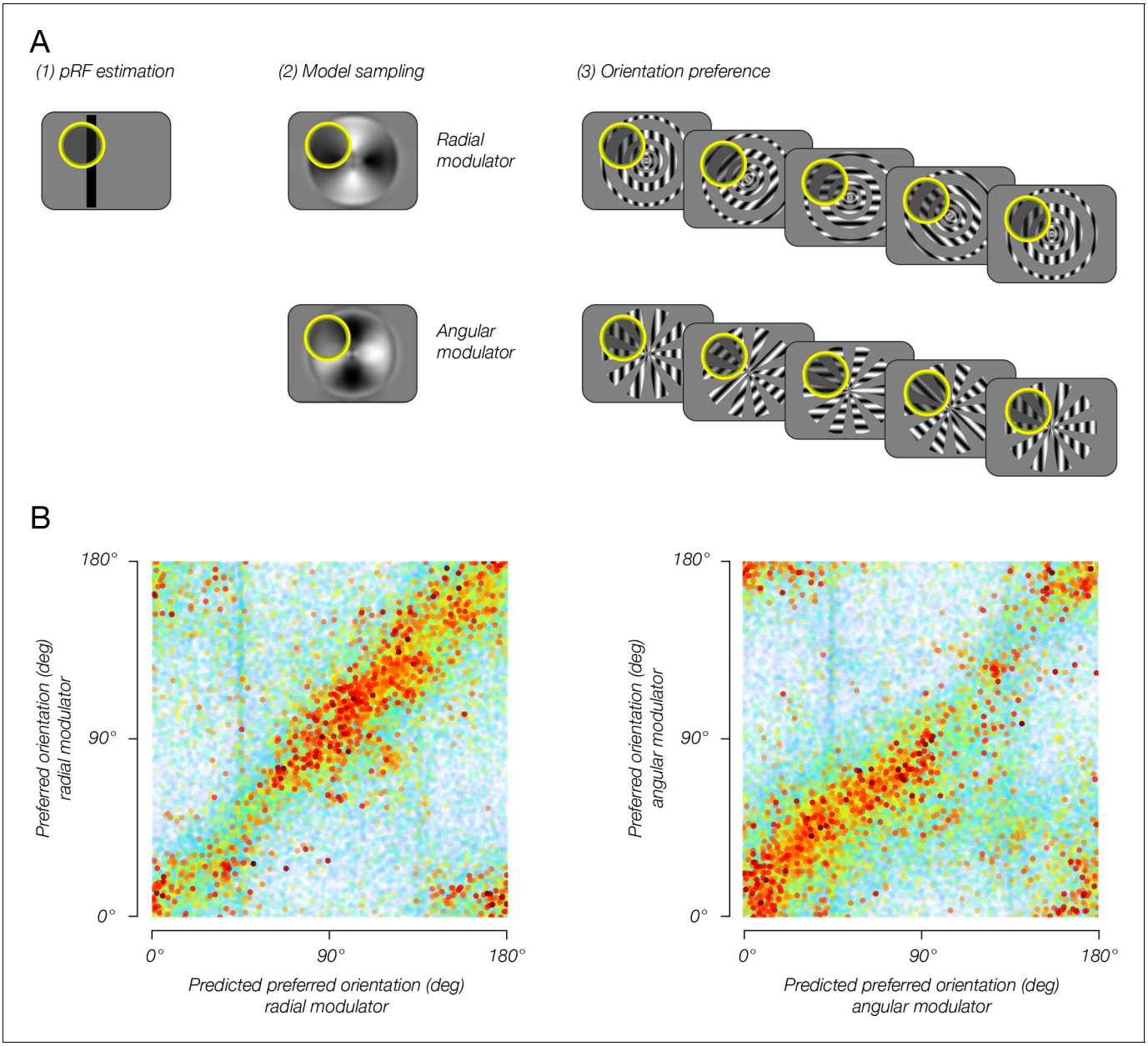

Figure 6. Combining the model with pRF estimates enables reliable predictions of single-voxel orientation preference. (**A**) pRF sampling method. (1) Each voxel's pRF was estimated based on an independent pRF-mapping scanning session. (2) Model output was sampled by the voxel pRF, resulting in an estimated preferred orientation for each modulator. (3) Estimated preferred orientation was compared to measured orientation preference, for each modulator. (**B**) Estimated orientation preference plotted against measured orientation preference. Sampling the model output with estimated pRFs yielded accurate predictions for each voxel's orientation preference for each of the two modulators, indicating that the model of stimulus vignetting provides a good account for the fMRI measurements of orientation preference.

DOI: https://doi.org/10.7554/eLife.37241.008

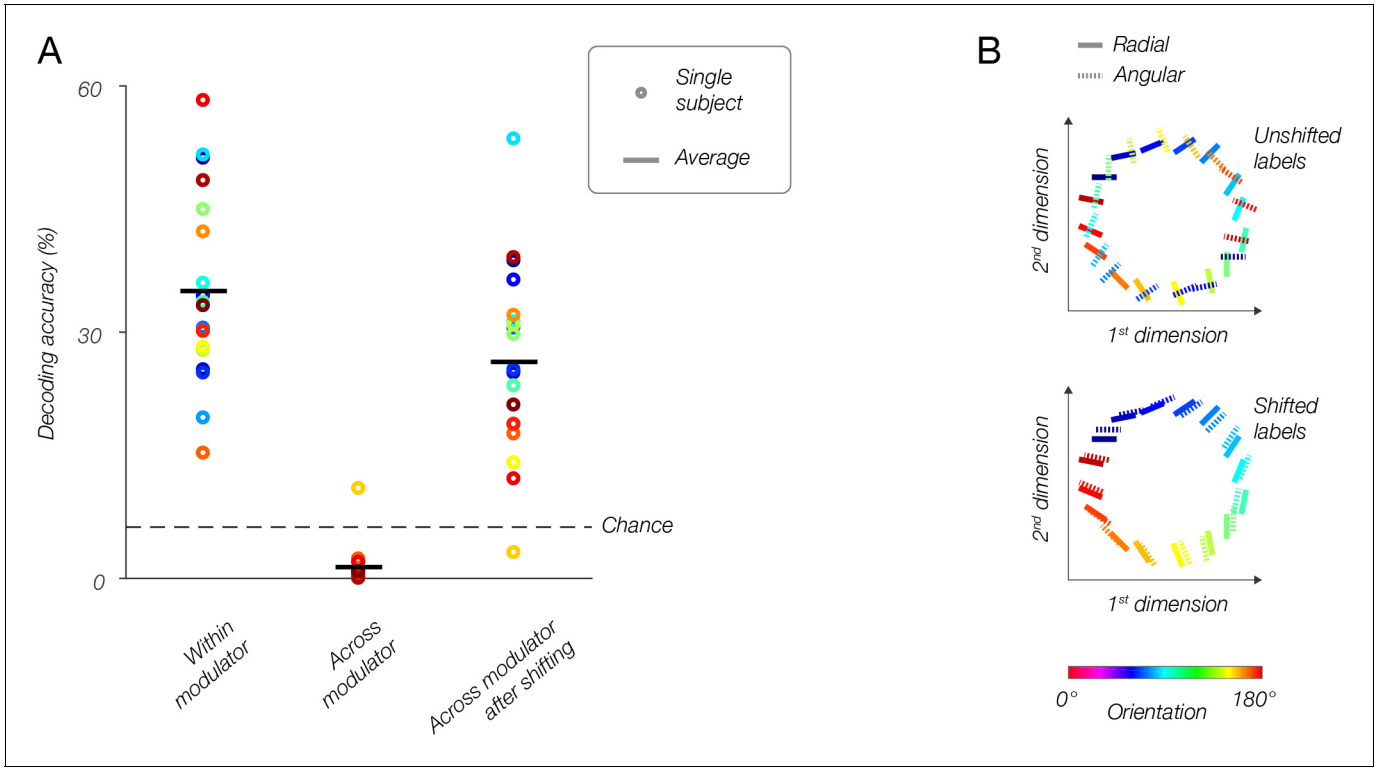

Figure 7. Population responses reflect the modulator, not stimulus orientation. (**A**) fMRI decoding. Within-modulator decoding: classifier was trained and tested on data from each modulator separately, in a leave-one-run-out cross-validation approach. Across modulator decoding: classifier was trained on data from one modulator and tested on data from the other modulator (and vice-versa). Across-modulator decoding after shifting: data for one modulator was shifted by 90˚, then the classifier was trained on that modulator and tested on the other (and vice-versa). (**B**) Multidimensional scaling. Top: population responses to all orientations for both modulators (solid lines, radial modulator; dotted lines, angular modulator) are plotted in 2D, such that distances between conditions reflect how different (i.e., dissimilarity = 1–r, where r is the correlation coefficient) the responses are. For the original data, orthogonal orientations from the two modulators have similar responses and are plotted near each other, while identical orientations taken from the two modulators evoked very different responses, and lay distant from each other. Bottom: after shifting the labels for the angular modulator by 90 deg, the two datasets align well, and similar orientations correspond to similar population responses regardless of the modulator.
DOI: https://doi.org/10.7554/eLife.37241.009